Fixed-point quantum circuits for quantum field theories

Natalie Klco [*] and Martin J. Savage [†]
Institute for Nuclear Theory, University of Washington, Seattle, Washington 98195-1550, USA

(Received 14 June 2020; accepted 19 October 2020; published 30 November 2020)

Renormalization group ideas and effective operators are introduced to efficiently prepare ground states of massive lattice field theories on digital quantum devices. This is accomplished with a systematic approximation through localized unitaries that removes an exponentially costly barrier in the spatial volume of the quantum simulation. With these methods, classically computed ground states in a spatial volume L, containing a few Compton wavelengths, can be used to determine operators for preparing the ground state toward the thermodynamic limit with a precision improving as e^{-mL} on beyond-classical quantum registers. Due to the exponential spatial decay of correlations in massive theories and the double exponential suppression of digitization artifacts in the number of qubits representing the scalar field, the derived fixed-point quantum circuits are expected to be relevant for simulations of quantum field theories throughout the evolution from small-scale near-term quantum devices to large-scale fault-tolerant quantum computers.

DOI: 10.1103/PhysRevA.102.052422

I. INTRODUCTION

Quantum field theories (QFTs) describing the properties and dynamics of fundamental particles and quantum many-body systems are anticipated to be addressed with analog quantum simulation and digital quantum computation [1–6]. In addition to being essential to scientific applications in nuclear physics, high-energy physics and basic energy sciences, the distributed quantum degrees of freedom of QFTs provide a framework underlying the design of large-scale quantum simulators and fault tolerant quantum computers. Numerical evaluations of QFTs typically involve discretizing space-time into a lattice of points on which matter fields are defined, with gauge fields defined on the links between grid points. Physical predictions can be derived from such calculations by extrapolating to the limit of infinite spatial or space-time volume and the continuum limit where the distance between grid points vanishes. This can be accomplished by computing in sufficiently large volumes with sufficiently fine discretizations, then extrapolating using known forms.

Preparing the ground state of a QFT Hamiltonian on digital quantum computers is challenging and has been identified as a leading contribution in estimates of the quantum resources required to simulate scattering in scalar field theory [2,3,5,7]. When digitizing a scalar field at each lattice site and employing nearest-neighbor or smeared nearest-neighbor finite difference operators in conjugate momentum space, induced systematic errors in observables depend polynomially on the field digitization spacing. However, the efficiency of the quantum Fourier transform performed on each site leads to a protection, encapsulated by the Nyquist-Shannon sampling theorem, resulting in a suppression of digitization artifacts from polynomial to nonperturbative exponential convergence [2,3,8–11].

Preparing an arbitrary real function with support across the Hilbert space of a quantum register requires the number of entangling gates to grow exponentially with the number of qubits. In the special case of a Gaussian profile, where the wave packet expands retaining its shape under time evolution, *Somma Inflation* can be used to transform a Gaussian with support localized in the Hilbert space to a Gaussian with support distributed throughout the Hilbert space without an exponential increase in the number of entangling gates [8]. While individual Gaussians are a start, the scalar field ground state correlates Gaussians on each spatial site determined by the gradient operator. Thus, introducing the spatial gradient operator creates entanglement among spatial sites, significantly increasing the number of entangling gates that are required to prepare the ground state [11–14]. As previously shown, the number of unitary operators (classified as single-qubit rotations controlled on the state of h other qubits with fixed maximum h) capable of fixed-precision ground state preparation scales linearly with the spatial volume in massive QFTs due to the exponential localization of classical correlations and entanglement [14]. It was found that the rotation angles (α angles) defining the unitary transformations become exponentially suppressed as the operators they define become increasingly nonlocal.

In this work, the properties of the ground states of noninteracting scalar field theories and the symmetries of the corresponding quantum circuits are exploited to derive spatially localized effective operators for initializing large instances of ground-state wave functions, defining analytic "fixed points" of the localizable quantum circuits. The systematic errors associated with these effective operators are shown to be exponentially suppressed with the field digitization. In analogy with effective operators used in effective field theories induced or renormalized by removing degrees of freedom,

[*] klcon@uw.edu
[†] mjs5@uw.edu

these effective operators are determined by integrating (tracing) over contributions from fields on lattice sites that are not involved in the controlled operations used to entangle the state on a given lattice site. The unitary transformations associated with these effective operators rapidly evolve toward fixed points as the number of sites integrated out becomes large. The implication is that systems of size commensurate with the correlation length, and which can be solved with classical computing resources, can be used to determine the controlled unitary rotation operations capable of preparing larger ground states on quantum computers than possible classically. This is also true for interacting scalar field theories.

II. SCALAR FIELD GROUND STATE

Working in the basis of eigenstates of the field operator $\hat{\phi}$ [2,3], the position-space, digitized wave function of a noninteracting massive lattice scalar field ground state mapped onto a quantum register, $|\Omega\rangle$ is

$$|\Omega\rangle = \sum_{\boldsymbol{\phi}} \psi(\boldsymbol{\phi})|\boldsymbol{\phi}\rangle, \quad \psi(\boldsymbol{\phi}) \propto e^{-\frac{1}{2}\boldsymbol{\phi}^T \mathbf{K}\boldsymbol{\phi}}, \tag{1}$$

where the sum over $\boldsymbol{\phi}$ extends over the values of the field at each site for every spatial site. This state can be prepared from the fiducial state operationally with a nonunitary operator $\hat{\Gamma}$

$$\hat{\Gamma} = e^{-\frac{1}{2}\hat{\boldsymbol{\phi}}^T \mathbf{K}\hat{\boldsymbol{\phi}}}, \quad |\Omega\rangle \propto \hat{\Gamma} H^{\otimes N}|0\rangle^{\otimes N}, \tag{2}$$

where H is the Hadamard gate. The wave function is sampled at regular intervals, δ_ϕ, between field truncations $\pm\phi_{\max}$ on each site of an N-site lattice with n_Q qubits per site [2,3,11]. Being constructed from the field operators $\hat{\phi}_x|\phi_x\rangle = \phi_x|\phi_x\rangle$ at the site x, $\hat{\Gamma}$ can be considered to be a finite dimensional operator with wave function amplitudes along the diagonal corresponding to those of the digitized infinite dimensional Hilbert space of continuous fields. An alternate identification of $\hat{\Gamma}$ satisfying the preparation requirement of Eq. (2) is the density matrix of the digitized ground state. Both perspectives will be useful in the identification of effective operators for the fixed-point circuit elements.

The symmetric matrix of sitewise correlations $\mathbf{K}$ is exponentially localized to the diagonal with the form e^{-mr}/r, the two-site mutual information falls, up to power law components, as e^{-2mr} with separation, and the negativity is localized at the ultraviolet length scale of the finite-difference momentum operator used to calculate $\mathbf{K}$ [14–16]. In explicit connection between the quantum circuitry necessary to prepare wave functions and their intrinsic correlations, we showed that the circuit operations to prepare the ground state of a massive scalar field can be localized [14]. This localization is controlled by the structure of $\mathbf{K}$. Specifically, we showed that if the $\mathbf{K}$ matrix of correlations for a periodic lattice is truncated to be a band-diagonal matrix with vanishing K_{0i} for $i > d$, then quantum circuit elements can be made to depend only on the state of neighboring sites to a maximum distance d [14]. This feature of the circuit prevails in spite of the nonzero mutual information extending beyond this radius. For clarity, in what follows the $\mathbf{K}$ truncation will be taken to be $d = 1$ unless otherwise noted and thus represent the largest contributions in the correlation hierarchy.

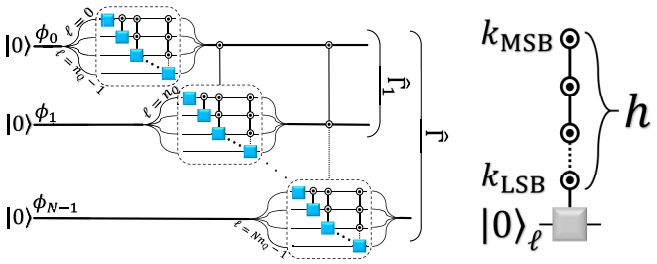

FIG. 1. Quantum circuit for preparing an arbitrary real wave function organized as quantum registers of n_Q qubits (dark horizontal lines) at each indexed field site ϕ_j. (right) The fundamental controlled rotation operator $R_y(\theta) = e^{-i\theta\sigma_y}$ acting on qubit ℓ and controlled on h previous qubits. The open-closed controls indicate a set of operators with unique angles $\theta_{\ell,k}$ controlled on each of the possible 2^h binary strings, k, with the most significant bit (MSB) at the top and the least significant bit (LSB) at the bottom.

In a massive noninteracting theory, a field redefinition can be performed to remove explicit mass dependence from the qubit representation, and a tuning of the field truncation, $\phi_{\max}$, can be performed to minimize digitization artifacts. In the case of an interacting theory, the coupling can broaden or narrow the field distribution, requiring a retuning of the field truncation. If the renormalized mass of the theory vanishes, the matrix $\mathbf{K}$ is no longer exponentially suppressed, and the analysis and circuit design in this work lose utility.

III. QUANTUM CIRCUITRY

By defining the structure of a quantum circuit, an implicit definition is made of the symmetries and wave function features that are naturally created upon implementation. Ideally, designed quantum circuits have structures that parallel those of the theory being simulated. This allows, for example, decaying correlation functions to manifest as a hierarchy of operators with distance in the qubit register. In the following, the circuit presented in Ref. [14] is first reviewed. Having established physical properties of the field embedded in this structure, the discussion will then extend to determining fixed-point circuit parameters for ground state preparations larger than could be explicitly represented on classical devices.

Operators used in the localizable circuits can be defined by three numbers: two indices and an angle, as shown at the right of Fig. 1. The angle defines the rotation operator about the y axis that acts on the target qubit. The two indices ℓ and k, define the target qubit index and the binary-interpreted integer value of the controls. Thus, declaring an angle of the form $\theta_{\ell,k}$ is equivalent to declaring a rotation operator along with its location and control values on previous qubits. The θ circuit shown in Fig. 1 contains each of the 2^ℓ controlled operators with differing values of k acting on each qubit, ordered by ℓ from smallest to largest. Operators with equal ℓ and differing k commute.

Linear combinations of these θ angles produce α angles with magnitudes exponentially suppressed in the spatial extent of the associated circuit element. In this sense, the α-angle operators are localized according to the classical two-point correlation function, and thus the exponentially decaying

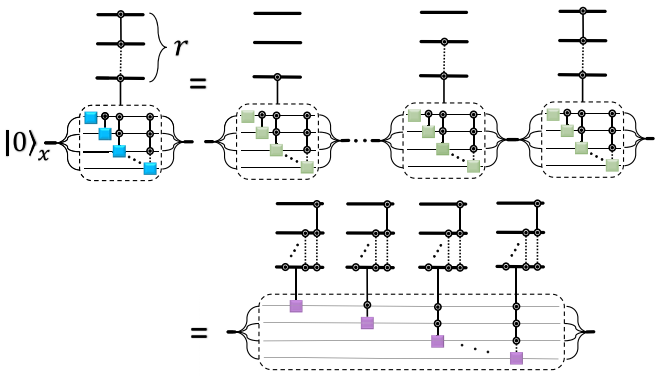

FIG. 2. Sitewise expansion of angles $\theta_{\ell,k}$, appearing in rotation operators represented as blue squares, into angles $\alpha_{\ell h,k}$ appearing in rotation operators represented by purple squares. Diagonal continuation dots represent the inclusion of controlled operators with every intermediate number of controls.

K [14]. These angles are denoted as $\alpha^{x,r}_{\ell h,k}$. The lower(upper) indices describe the associated controlled rotation at the level of qubits(sites). There is a many-to-one relationship between the qubit and site indices, respectively. For the qubit indices, ℓ and k remain as defined for the θ angles. The additional index h is the "height" of the operator or number of controls. For the θ circuit, all operators are defined to have $h = \ell$. This equivalence between the operator height and its distance from the top of the qubit register is lifted for the α circuit in order to allow systematic localization of the operators and the relation becomes $k_{\max} = 2^h - 1$. For the site indices, x is the site number at which the rotation acts and r is the site distance spanned by the operator. These indices are connected by $x = \lfloor \ell/n_Q \rfloor$ and $r = \lfloor h/n_Q \rfloor$, where $\lfloor y \rfloor$ denotes the floor of y.

The sitewise α transformations are defined by expanding a θ operator extending over multiple sites defined by angles $\vec{\theta}^x_\ell$ into rotations over a truncated number of sites with $h = \{\ell - (x-1)n_Q, \ldots, \ell - n_Q, \ell\}$ respectively being at physical distances $r = \{1, \ldots, x\}$. This process is shown diagrammatically in Fig. 2. At the left is a site-rotation controlled on the field at the r previous sites. It is desirable to isolate the sensitivity to controls at small spatial distance if the target wave function has localized correlations. This is shown diagrammatically with the green circuit at the right of Fig. 2 where site rotations controlled at short distances are extracted from those controlled at long distances. A locality truncation removes circuit elements beginning at the right end of this circuit. In the second line of this diagram, the purple circuit has grouped operators acting on a particular qubit. Due to noncommutativity of rotations and controls, these angles are distinct from those of the previous expansion. It is the angles of the latter, purple circuit $\alpha^{x,r}_{\ell h,k}$ that are naturally related to the $\theta_{\ell,k}$ on the left through simple linear combinations and averaging [14]. The α angles for such decompositions with **K** truncated at $d = 1$ are equivalent to the θ angles at distances 1, and vanishing for operators of greater spatial extent

$$\alpha^{x,r}_{\ell h,k} = \begin{cases} \theta^x_{\ell,k} & r = 1 \\ 0 & r > 1 \end{cases} . \tag{3}$$

This supports the statement that the α angles are controlled by the **K** matrix, exponentially suppressed in spatial locality controlled by the mass of the lightest particle.

The nature of these quantum circuits used to prepare the digitized ground state is such that adding qubits to increase the density of states between the upper and lower values of the field at each site changes the number and values of the angles associated with the unitary operations. The additional field samples with each added qubit are interleaved with those at the previous field digitization, leading to a direct connection between the last qubit in each site and the high conjugate momentum modes. With increasing n_Q, θ angles associated with the last qubit in each site tend towards a constant value of $\pi/4$, the angle for which additional samples are simply copies of their lower-digitization-scale predecessors. This is a natural phenomena associated with the wave function being smooth or defined by an upper-bounded Fourier space. In the circuit language, if n_Q is taken to be large, the $\theta_{jn_Q-1,k}$ angles tend to $\pi/4$ for all integer $j \in \{1, \ldots, N\}$ and $k \in \{0, \ldots, 2^{jn_Q-1} - 1\}$. In the translation to localizable α angles shown in Fig. 2, these long-distance controlled θ operators tend towards a single-qubit α operator $R_y(\pi/4)$ on the last qubit (the same effect as acting with the Hadamard gate for state $|0\rangle$). The α angles thus demonstrate a localization not only in spatial distance from exponentially decaying spatial correlation functions, but also within the sites due to the hierarchy of conjugate momentum modes. In contrast, operators acting on early qubits in the digitization (associated with the low conjugate momentum modes) yield rotation angles that tend to a fixed, nonconstant distribution as a function of the field values on controlled sites above. Given the expectation that small values of $n_Q \leqslant 5$ will be sufficient for foreseeable calculations of the massive scalar field on quantum hardware, the following will be focused on fixed n_Q, where angles defining local operators evolve to fixed points as the number of spatial sites in the lattice becomes large. Thus, for preparing lattices containing many correlation lengths, the number of unique local operators becomes independent of the lattice volume.

IV. FIXED-POINT CIRCUIT

For the particular case of the θ circuit (see Fig. 1) where the state is prepared with asymmetric operations, the rotations on each site are dependent on the site register above the site on which the rotation acts. The associated θ angles can be calculated from the ratio of sums of squared amplitudes in the wave function, marginalizing over the field on lower sites. By considering partitions of the wave function at levels corresponding to the binary hierarchy of the qubits in the register, the θ angles can be directly calculated, shown in Ref. [13], as

$$\theta^x_{\ell,k} = \arctan \sqrt{\frac{\sum_{j=0}^{2^b-1} \langle \psi_n | \hat{\Gamma}^{2,\mathrm{eff}}_x | \psi_n \rangle}{\sum_{j=0}^{2^b-1} \langle \psi_d | \hat{\Gamma}^{2,\mathrm{eff}}_x | \psi_d \rangle}} . \tag{4}$$

The states in the numerator and denominator are

$$\begin{aligned} |\psi_n\rangle &= |\phi(\kappa^{\phi_{x-1}}), \quad \phi(2^{b+1}\kappa^{\phi_x} + 2^b + j)\rangle, \\ |\psi_d\rangle &= |\phi(\kappa^{\phi_{x-1}}), \quad \phi(2^{b+1}\kappa^{\phi_x} + j)\rangle, \end{aligned} \tag{5}$$

where $\phi(\kappa^{\phi_x}) \equiv \phi(x;\kappa^{\phi_x})$ denotes the field value at digitization address κ^{ϕ_x} at site x

$$\phi(\kappa^{\phi_x}) = \phi_{\max} - \delta_\phi \kappa^{\phi_x} \quad . \tag{6}$$

The site index and inner-site qubit index are

$$x = \left\lfloor \frac{\ell}{n_Q} \right\rfloor, \quad b = (n_Q - 1) - \ell \bmod n_Q \quad , \tag{7}$$

where the latter describes the location of the rotation within the site x by the number of qubits back it acts from the last qubit in the site. This is equal to the number of qubits within the site, but below the rotation, that need be additionally marginalized from the calculation. The index k has been interpreted in binary and grouped for its localization at each site of the scalar field

$$k = \{\kappa^{\phi_0}, \kappa^{\phi_1}, \ldots, \kappa^{\phi_{x-1}}\}_2 \quad . \tag{8}$$

The sitewise κ^{ϕ_n} index takes values in the range $\{0, \ldots, 2^{n_Q} - 1\}$.[1] The effective operator, $\hat{\Gamma}^{2,\text{eff}}_x$, relevant for calculating θ at site x is a marginalization of $\hat{\Gamma}^2$ over the field values of all sites beneath the rotation location x,

$$\begin{aligned} \hat{\Gamma}^{2,\text{eff}}_x &= \text{Tr}_{\boldsymbol{\phi}_>}[\hat{\Gamma}^2], \\ \boldsymbol{\phi}_> &= \{\phi_{x+1}, \phi_{x+2}, \ldots, \phi_{N-1}\}. \end{aligned} \tag{10}$$

Note that the reduced $\hat{\Gamma}^{2,\text{eff}}_x$ operator marginalizes in the probabilities, not the amplitudes. This is a manifestation of the use of y axis rotations in the circuit construction, producing trigonometric functions of the rotation angles in the wavefunction amplitudes. Sums over squares of these amplitudes then sequentially remove qubits from the end of the register. In terms of the qubit reduced density matrix, the angles are defined by ratios of the diagonal matrix elements

$$\theta_{\ell,k} = \arctan \sqrt{\frac{\langle 2k+1|\hat{\rho}_\ell|2k+1\rangle}{\langle 2k|\hat{\rho}_\ell|2k\rangle}} \quad , \tag{11}$$

with $\hat{\rho}_\ell$ the ground state reduced density matrix of the first $\ell + 1$ qubits

$$\hat{\rho}_\ell = \text{Tr}_{q>\ell}[\hat{\rho}] \quad . \tag{12}$$

By marginalizing at the qubit level [rather than at the site level as done in Eq. (4)], the sums in the numerator and denominator over the 2^b values of the field at higher digitization frequency in the site x are handled in the trace reduction of the density matrix. For the current application of initializing the ground state, the operator definition in Eq. (2) is more efficient for the construction of local effective operators.

The number of θ angles required to prepare the ground state associated with $\hat{\Gamma}$ has super-polynomial scaling in the number of lattice sites on the full quantum register. However, the α angles, which can be derived from $\hat{\Gamma}^{2,\text{eff}}_x$, grow in number superpolynomially with respect to the lattice sites within a few Compton wavelengths—parametrically smaller than that of $\hat{\Gamma}$. It is this reduction that enables a classical computation to inform state preparation on beyond-classical quantum registers to a fixed precision.

If the qubit registers in the lower region of the circuit are taken to be continuous fields without field truncation,

$$\hat{\Gamma}^{2,\text{eff}}_x \to \int_{\boldsymbol{\phi}_>} \hat{\Gamma}^2 \propto e^{-\hat{\boldsymbol{\phi}}^T_\leqslant \mathbf{K}_{x+1} \hat{\boldsymbol{\phi}}_\leqslant + K^2_{01} \frac{\det \mathbf{K}_{\bar{x}-1}}{\det \mathbf{K}_{\bar{x}}} \hat{\phi}^2_x}, \tag{13}$$

where $\mathbf{K}_n$ is the first $n \times n$ sub-block in $\mathbf{K}$ and $\bar{x} = N - (x+1)$ is the number of sites below site x (the number of sites in $\phi_>$). Note that for the calculation of θ angles with $\mathbf{K}$ truncation at $d = 1$, the field values above $\hat{\phi}_{x-1}$ may be ignored as they cancel in the ratio in Eq. (4). In this scenario, the effective operator reduces to a local operator

$$\hat{\Gamma}^{2,\text{eff}}_x \propto e^{-K_{00}\hat{\phi}^2_{x-1} - 2K_{01}\hat{\phi}_{x-1}\hat{\phi}_x} e^{-(K_{00} - K^2_{01}\frac{\det \mathbf{K}_{\bar{x}-1}}{\det \mathbf{K}_{\bar{x}}})\hat{\phi}^2_x}. \tag{14}$$

This operator captures the effective $\mathbf{K}$ matrix of correlations relevant for the unitaries acting at site x, integrating out degrees of freedom in a manner resembling the renormalization group. With $d > 1$, the effective operator remains exponentially localized with the structure of $\mathbf{K}$. The ratio of determinants tends to a constant at large lattice sizes ($N \to \infty$), and can be expressed for continuous $\bar{x}$ fields as

$$\frac{\det \mathbf{K}_{\bar{x}-1}}{\det \mathbf{K}_{\bar{x}}} = \frac{2}{K_{00} + \eta\left(1 + \frac{2}{-1 + (K_{00} - \eta)^{-\bar{x}}(K_{00} + \eta)^{\bar{x}}}\right)}, \tag{15}$$

$$\xrightarrow[\bar{x}\to\infty]{} \frac{2}{K_{00}\left(1 + \sqrt{1 - \frac{4K^2_{01}}{K^2_{00}}}\right)}, \tag{16}$$

with $\eta = \sqrt{K^2_{00} - 4K^2_{01}}$. At large volumes, these two elements of the correlation matrix are

$$K^\infty_{00} = \frac{2\sqrt{4+m^2}}{\pi} E\left(\frac{4}{4+m^2}\right) \quad , \tag{17}$$

$$\begin{aligned} K^\infty_{01} = {} & \frac{\sqrt{4+m^2}}{3\pi} \\ & \times \left[m^2 K\left(\frac{4}{4+m^2}\right) - (2+m^2) E\left(\frac{4}{4+m^2}\right)\right], \end{aligned} \tag{18}$$

where K and E are the complete elliptic integrals of the first and second kind, respectively. Having analytic forms of the asymptotic $\mathbf{K}$ matrix elements and determinant ratio is a convenient but unnecessary feature of the noninteracting scalar field. They are computationally inexpensive and can be easily calculated for large volumes.

The determination of fixed-point circuit elements has occurred in the limit of infinite volume, infinite field truncation $\phi_{\max}$, and continuous quantum registers on marginalized lattice sites of the field. Leading corrections to the above expressions due to the finite extent of the lattice scale as $O(e^{-mN})$ up to polynomial factors scaling approximately as $1/\sqrt{N}$. To quantify the systematic uncertainties associated with assumed continuous quantum registers, consider the distribution upon marginalization of the field at a single lattice

[1] As an example, for $n_Q = 2$, $x = 2$, and $k = 6$,

$$k = 6 = 0110 = \{1, 2\}_2 \quad , \tag{9}$$

such that $\kappa^{\phi_0} = 1$ and $\kappa^{\phi_1} = 2$. Thus the control of $k = 6$ is associated with the scalar field on sites 0 and 1 of $\phi_0 = \phi_{\max} - \delta_\phi$ and $\phi_1 = \phi_{\max} - 2\delta_\phi$.

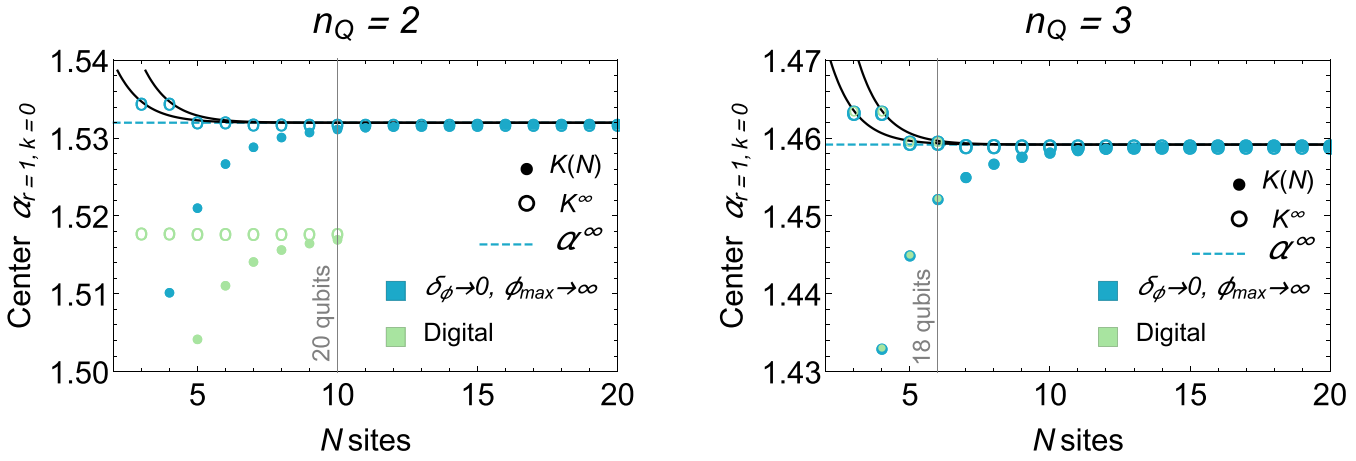

FIG. 3. Evolution of an angle associated with a localized operator at the center of the lattice, $\alpha(x = \lfloor \frac{N}{2} \rfloor, r = 1, \ell = n_Q(\lfloor \frac{N}{2} \rfloor + 1) - 1, h = 2n_Q - 1, k = 0)$, with lattice size N. The scalar field is defined by $m = 0.3$, truncated in correlations at K_{01}, and truncated for digitization with maximum field value $\phi_{\max} = 3.5$. Blue points are the results of calculations approximating sites in the second half of the lattice to be continuous fields ($\delta_\phi \to 0$) without field truncation ($\phi_{\max} \to \infty$). Green points are the results of calculations within a digitized and truncated qubit representation. Closed circles indicate the **K** matrix scales with system size $[K(N)]$, while open circles indicate that the infinite-volume **K** matrix elements are used (K^∞). The solid black lines show the N dependence of the continuum calculations with infinite-volume **K** matrix elements, while the blue dashed line is the fixed-point angle (α^∞) calculated for continuum sites in the lower half lattice in the limit of infinite volume.

site,

$$\mathcal{B}_1(\phi_\ell) = \sum_{\phi_c} e^{-(K_{00}\phi_c^2 + 2K_{01}\phi_\ell\phi_c)} \quad . \tag{19}$$

Utilizing Poisson resummation to relate the ϕ symmetrized Dirac comb, producing digitized field samples, to a sum over its Fourier modes, deviations are found to be exponentially suppressed with the field digitization,

$$\mathcal{B}_1^\infty(\phi_\ell) = \sqrt{\frac{\pi}{K_{00}\delta_\phi^2}} e^{\frac{K_{01}^2\phi_\ell^2}{K_{00}}} \times \left[1 + 2\sum_{n>0} e^{-\frac{n^2\pi^2}{K_{00}\delta_\phi^2}} \cos\left(n\pi\left(1 + \frac{2K_{01}\phi_\ell}{K_{00}\delta_\phi}\right)\right)\right], \tag{20}$$

where the term in brackets can written as an elliptic theta function. For fields digitized onto qubits with $\delta_\phi = \frac{2\phi_{\max}}{2^{n_Q}-1}$, the deviations from the continuum scale as $O(e^{-2^{2n_Q}})$, double exponentially in the number of qubits.

This rapid convergence is another manifestation of the Nyquist-Shannon sampling theorem, the effects of which can be seen in Fig. 3, where the convergence of a rotation angle in the center of the lattice is shown. The green points have been calculated through representation of the 2^{Nn_Q} dimensional digitized wave function for systems of up to 20 qubits. The blue points have had the effective operator replaced by the continuum and untruncated (in $\phi_{\max}$) effective operator of Eq. (14). As such, the N dependence of the blue closed points comes from the determinant ratio in Eq. (15) and the N dependence of the **K** matrix itself. If the infinite volume values of **K**, as shown in Eqs. (17) and (18), are used, the open points and black lines are recovered, demonstrating a rapid convergence to the continuum angles. The continuum values, α^∞, are shown as blue dashed lines which are calculated by defining the effective operator with Eqs. (16), (17), and (18).

On the left panel of Fig. 3, a coarse qubit digitization of $n_Q = 2$ is used on each site. The angle calculated in the continuum without field truncation agrees with that calculated in the digitized space to ∼1%. Thus substituting the fixed-point α angles for the digitized circuit provides sufficiently precise determinations of rotation angles necessary for initializing the ground state on even small instances of near-term quantum devices (where this precision matches that expected on hardware). Due to the double exponential convergence in the number of qubits used to digitize the field, increasing n_Q to three qubits (right panel of Fig. 3) shows good agreement between the angles defining the continuum and digitized circuits. Differences of angles in small volumes, where wave functions can be represented classically, are found to be ∼0.001%. While increasing n_Q requires additional circuit operations to prepare the ground state (see Fig. 2), the number of gates, $O(N2^{2n_Q})$, grows more slowly than the ability to improve them. The double exponential convergence in digitization artifacts implies that increasing n_Q, and thus the fidelity of the wave function, parametrically improves the fidelity-to-gate ratio when using fixed-point circuits to initialize the scalar field ground state.

As the distance truncation, d, of **K** is raised, the effective operator relevant for calculating the θ angles at a particular site becomes less local. The modification to the reduced **K** matrix in the effective operator is generally

$$\hat{\Gamma}^{2,\text{eff}} \propto e^{-\phi_{\leqslant}^T (A - BC^{-1}B^T)\phi_{\leqslant}} \quad , \tag{21}$$

with

$$\mathbf{K} = \left(\begin{array}{c|c} A & B \\ \hline B^T & C \end{array}\right), \quad [A] = (x+1)(x+1). \tag{22}$$

It can be seen that the correction to the site-site correlations in the effective operator, $BC^{-1}B^T$, is nonzero only in the lower

subblock of dimension d controlled by the largest nonzero K_{0d} retained in **K**. This is consistent with the physical intuition that the off-diagonal elements of **K** control the site distance of communication throughout the lattice. This localization to the lower subblock is also connected to the localization of the effective operator(s) necessary to calculate θ angles defining the fixed-point circuit.

V. REFLECTIONS

In this work, fixed-point quantum circuits have been introduced for the preparation of the noninteracting scalar field ground state on digital quantum hardware. Determining the circuit elements necessary to initialize large instances of the quantum field requires classical computational resources scaling only with the spatial distance of correlations. For the massive scalar field, these correlations decay exponentially with distance, leading to the ability to determine fixed-point circuits for preparing the ground state on quantum devices for larger lattices than could be stored classically. This technique is also applicable to interacting scalar field theory.

In this work, the continuum limit (decreasing lattice spacing) has not been considered. Taking this limit is required to make predictions for physical observables with a complete quantification of uncertainties. As the lattice spacing is reduced, the number of lattice sites within a correlation volume increases. This scaling is power law with the lattice spacing. The fixed-point analysis that we have presented remains valid, but with an increased number of required α angles.

In leveraging the entanglement structure of the represented quantum state for computational advantage, the fixed-point circuitry is reminiscent of the powerful techniques of tensor networks [17–20]. A notable distinction is that entanglement information of a fixed-point circuit is not stored locally in a bond dimension, rather it is stored nonlocally at natural distances set by the classical correlation length scale. Though daunting with tensor network approaches [21–23], it is expected that the resulting volume independence of calculating the fixed-point circuitry will persist beyond one spatial dimension, as long as correlations are localized in each direction. It is plausible that a hybrid framework leveraging tensor network methods may provide an effective way to access the α angles using classical computing.

In contrast to adiabatic state preparation techniques, there is no dynamic evolution or convergence process required of a quantum device for an initialization using fixed-point circuitry. This methodology is likely to be limited for massless fields, where the exponential localization of the **K** matrix is lost, and impractical when light masses or small lattice spacing causes the correlation volume to exceed classical computing capabilities. In particular, the systematic uncertainty introduced into the quantum simulation by the finite classical volume of spatial extent L will scale as $\sim e^{-mL}$, unless nonperturbatively modified by discretization effects, for example, Refs. [24,25].

While it is conceived that the ground state of an interacting theory can be initialized beginning from the noninteracting ground state adiabatically, there is no barrier to applying these fixed-point methods to interacting ground states as well. This provides an alternative state preparation mechanism that avoids additional circuit depth scaling with unpredictable spectral gaps throughout the dynamical adiabatic process. While such applications evade analytic solution, both perturbative corrections to the circuit elements and nonperturbative analyses can be performed. The perturbative approach leverages the analytic control demonstrated here in defining the noninteracting state preparation circuit, though further exploration is necessary to understand the corrections when interactions are strong. Alternatively, it is viable to inform fixed-point circuits for interacting ground states nonperturbatively. Infinite volume limits of circuit elements can be reliably extrapolated from finite volume calculations capturing only the exponentially localized correlation length scale. With currently available classical supercomputing resources, α angles can be determined for a range of lattice spacings, masses and couplings, that will enable ground state preparation on future quantum computers—a necessary though insufficient ingredient for quantum advantage. Already in the NISQ era, with 50–100 qubits, this formulation will be useful in benchmarking simulations of field theories.

Fixed-point quantum circuits are expected to be relevant for initializing the ground states of fields defined by locally-interacting massive particles with exponentially decaying correlation functions or area-law entanglement. It is further anticipated that confining gauge theories will admit fixed-point quantum circuits, suggesting how classical calculations of the QCD vacuum could inform state preparation on beyond-classical quantum devices.

ACKNOWLEDGMENTS

We would like to thank Aidan Murran for inspiring interactions. N.K. and M.J.S. were supported by the Institute for Nuclear Theory with DOE Grant No. DE-FG02-00ER41132, and Fermi National Accelerator Laboratory PO No. 652197. This work is supported in part by the US Department of Energy, Office of Science, Office of Advanced Scientific Computing Research (ASCR) quantum algorithm teams program, under field work Proposal No. ERKJ333. N.K. was supported in part by a Microsoft Research PhD Fellowship.

[1] R. P. Feynman, Int. J. Theor. Phys. **21**, 467 (1982).
[2] S. P. Jordan, K. S. M. Lee, and J. Preskill, Science **336**, 1130 (2012).
[3] S. P. Jordan, K. S. M. Lee, and J. Preskill, Quant. Inf. Comput. **14**, 1014 (2014).
[4] S. P. Jordan, K. S. M. Lee, and J. Preskill, arXiv:1404.7115.
[5] S. P. Jordan, H. Krovi, K. S. M. Lee, and J. Preskill, Quantum **2**, 44 (2018).
[6] M. C. Bañuls *et al.*, Eur. Phys. J. D **74**, 165 (2020).
[7] A. Kitaev and W. A. Webb, arXiv:0801.0342.
[8] R. D. Somma, Quantum Inf. Comput. **16**, 1125 (2016).
[9] A. Macridin, P. Spentzouris, J. Amundson, and R. Harnik, Phys. Rev. Lett. **121**, 110504 (2018).
[10] A. Macridin, P. Spentzouris, J. Amundson, and R. Harnik, Phys. Rev. A **98**, 042312 (2018).
[11] N. Klco and M. J. Savage, Phys. Rev. A **99**, 052335 (2019).

[12] K. Yeter-Aydeniz, E. F. Dumitrescu, A. J. McCaskey, R. S. Bennink, R. C. Pooser, and G. Siopsis, Phys. Rev. A **99**, 032306 (2019).
[13] N. Klco and M. J. Savage, Phys. Rev. A **102**, 012612 (2020).
[14] N. Klco and M. J. Savage, Phys. Rev. A **102**, 012619 (2020).
[15] M. Srednicki, Phys. Rev. Lett. **71**, 666 (1993).
[16] K. Audenaert, J. Eisert, M. B. Plenio, and R. F. Werner, Phys. Rev. A **66**, 042327 (2002).
[17] S. R. White, Phys. Rev. Lett. **69**, 2863 (1992).
[18] G. Vidal, Phys. Rev. Lett. **91**, 147902 (2003).
[19] U. Schollwöck, Rev. Mod. Phys. **77**, 259 (2005).
[20] F. Verstraete, V. Murg, and J. I. Cirac, Adv. Phys. **57**, 143 (2008).
[21] F. Verstraete and J. I. Cirac, arXiv:cond-mat/0407066.
[22] F. Verstraete, M. M. Wolf, D. Perez-Garcia, and J. I. Cirac, Phys. Rev. Lett. **96**, 220601 (2006).
[23] N. Schuch, M. M. Wolf, F. Verstraete, and J. I. Cirac, Phys. Rev. Lett. **98**, 140506 (2007).
[24] S. Marcovitch, A. Retzker, M. B. Plenio, and B. Reznik, Phys. Rev. A **80**, 012325 (2009).
[25] N. Klco and M. J. Savage, arXiv:2008.03647.